

Model and Attitude Control of a Miniature Hybrid Autogyro

Ziwei Song, Zhihao Cai, Kunpeng Li, Jiang Zhao and Ningjun Liu

1 Introduction

Hybrid layout UAV is a new direction of the future development of UAV, which has several flight patterns and is different from the traditional aircraft. This kind of UAV has the abilities of both short takeoff and landing and cruising on high speed through the conversion between different flight patterns.

As we know, autogyro can fly at very low speeds, and have good short takeoff and landing (STOL) performance [1]. But at the same time, the rotor structure is also limited its flight performance in high-speed regimes. During high-speed flight, high autorotation speeds cause such problems as retreating blade stall, blade tip shock waves and excess vibration, similar to those experienced in helicopters [2]. A way of improving the autogyro's high-speed flight performance is to use a hybrid autogyro configuration, in which fixed wings are added to the autogyro. At low flight speeds, the rotor provides most of the lift, thus retaining the autogyro's STOL performance. At high flight speeds, some of the lift is generated by the fixed wings, and rotor load is reduced [3].

In short, the hybrid autogyro has excellent overall performance. However, domestic and foreign research on such hybrid autogyro is rare, the study of its flight control is rarely reported. In this paper, for the strong coupling, nonlinear and time-varying characteristics of the system, we designed attitude controller based on back-stepping strategy.

Z. Song (✉) · Z. Cai (✉) · K. Li · J. Zhao · N. Liu
School of Automation Science and Electrical Engineering, Beihang University,
100191 Beijing, China
e-mail: szwer1015@163.com

Z. Cai
e-mail: czh@buaa.edu.cn

2 Aircraft Dynamics Modelling

2.1 *The Structure of the Hybrid Autogyro*

The hybrid autogyro is built based on a Hobbyking Super-G RC autogyro. Wings from an RC glider are attached to the autogyro's fuselage, as shown in Fig. 1.

The main structure to obtain the lift of the hybrid autogyro is the non-powered rotating rotor (relies on the relative flow of the rotor to rotate the rotor, which is different from the way of the helicopter to drive the rotor) and the wing. The rotating rotor also could be tilted left and right for roll control. Pitch and yaw controls are achieved via the elevator and rudder. At this stage, the role of the wing is only to provide lift, using aileron for hybrid control does not be involved [4].

The establishment of a reasonable and accurate mathematical model is the basis for the design of the control law. In the paper, the rotor model, the fixed-wing model are estimated respectively, and then we can get the motion equation of the UAV. Aircraft parameters are shown in Table 1.

2.2 *Establish the Mathematical Model for the Hybrid Autogyro*

In the paper, we use the model structure shown in Fig. 2, calculate the force and moment of each part separately and the aerodynamic interference between the various parts should be considered.



Fig. 1 Hybrid autogyro

Table 1 Parameters of the aircraft

Parameters	Value	Unit
Mass	1.823	kg
Length	1.223	m
Rotor diameter	1.08	m
Blade length	0.518	m
Blade chord length	0.05	m
Wing span	0.74	m
Wing chord length	0.11	m
Horizontal tail area	0.08	m ²
Vertical tail area	0.075	m ²
I_x	0.0646	kg m ²
I_y	0.134	kg m ²
I_z	0.1265	kg m ²
I_{xz}	-0.017	kg m ²

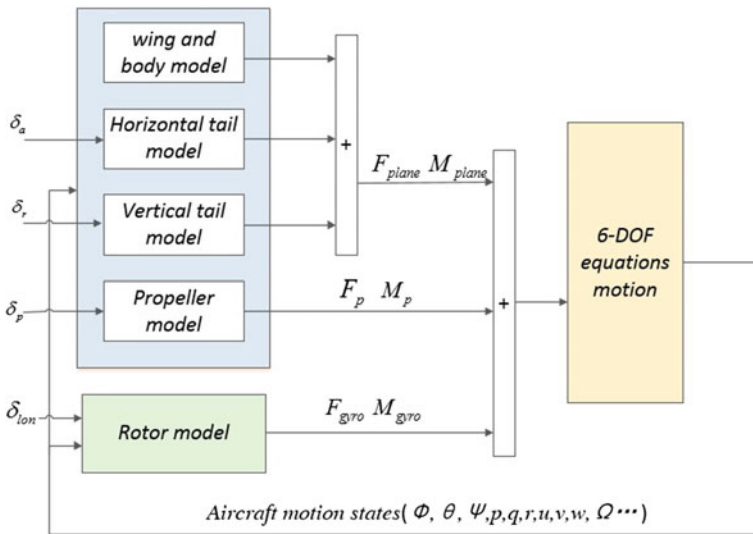


Fig. 2 Aircraft dynamics model structure

2.2.1 Rotor Model

When the hybrid autogyro flies forward, the paddle tilt backward, the flow relative to the UAV flow from the bottom up to the paddle, shown in Fig. 3.

In the diagram, α_R is the angle of the plane of the rotor. In order to establish the mathematical model of the rotor, we first use the leaf element theory to analyse the rotor's dynamics characteristic. The coordinate system used in this paper is

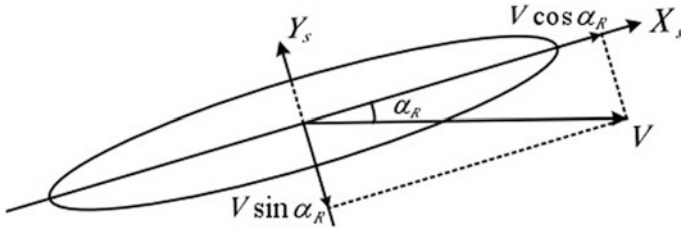


Fig. 3 Relative flow to the rotor when the aircraft flies forward

American coordinate system, and then we can get the force and moment of the rotor in the body coordinate system [5, 6].

$$\begin{cases} F_{xb-gyro} = -H \cos(\alpha_{1s} + \alpha_0) - T \sin(\alpha_{1s} + \alpha_0) \\ F_{yb-gyro} = T \sin b_{1s} - H \sin \beta \\ F_{zb-gyro} = -T \cos(\alpha_{1s} + \alpha_0) + H \sin(\alpha_{1s} + \alpha_0) \\ L_{gyro} = (T \sin b_{1s} - H \sin \beta)l_z + Q \sin(\alpha_{1s} + \alpha_0) \\ \quad + [-T \cos(\alpha_{1s} + \alpha_0) + H \sin(\alpha_{1s} + \alpha_0)]l_y \\ M_{gyro} = (-H \cos(\alpha_{1s} + \alpha_0) - T \sin(\alpha_{1s} + \alpha_0))l_z \\ \quad - (-T \cos(\alpha_{1s} + \alpha_0) + H \sin(\alpha_{1s} + \alpha_0))l_x - Q \sin b_{1s} \\ N_{gyro} = (T \sin b_{1s} - H \sin \beta)l_x - (-H \cos(\alpha_{1s} + \alpha_0) \\ \quad - T \sin(\alpha_{1s} + \alpha_0))l_y + Q \cos(\alpha_{1s} + \alpha_0) \cos b_{1s} \end{cases} \quad (1)$$

In the Eq. (1), T, H, Q are the lift force, the horizontal force and the anti-torque produced by the rotor, shown in Eq. (2). α_0 is the initial chamfering angles of the rotor paddle; α_{1s}, b_{1s} are the rotor longitudinal paddle inclination and horizontal paddle inclination, respectively. l_x, l_y, l_z is the coordinate of the center of the rotor paddle in the body coordinate system.

$$\begin{aligned} T &= C_T \rho S_{rotor} (\Omega R)^2 \\ H &= C_H \rho S_{rotor} (\Omega R)^2 \\ Q &= C_Q \rho S_{rotor} (\Omega R)^2 R \end{aligned} \quad (2)$$

The rotor speed can also reflect the flight status of the aircraft, so we also take the rotor speed as a state, the dynamic equation of the rotor rotation is:

$$\dot{\Omega} = -Q/J_{rotor} \quad (3)$$

2.2.2 Fixed-Wing Model

The fixed-wing part of the hybrid autogyro is essentially a fixed-wing aircraft, and can be modelled using well-established methods [7]. The forces and moments (in the aircraft body axes) of the entire fixed-wing part of the hybrid autogyro are:

$$\begin{aligned}
 \begin{bmatrix} F_{x_fw} \\ F_{y_fw} \\ F_{z_fw} \end{bmatrix} &= \begin{bmatrix} C_{x_b} \\ C_{y_b} \\ C_{z_b} \end{bmatrix} q_b S_b + R_{b/a} \begin{bmatrix} C_{x_w} \\ C_{y_w} \\ C_{z_w} \end{bmatrix} q_w S_w \\
 &+ R_{b/ht} \begin{bmatrix} -C_{x_d\epsilon} \\ 0 \\ C_{y_d\epsilon} \end{bmatrix} S_{ht} q_{ht} + R_{b/vt} \begin{bmatrix} -(C_{d_vt} + C_d^{\delta_r}) \\ C_{l_vt} + C_l^{\delta_r} \\ 0 \end{bmatrix} S_{vt} q_{vt} \\
 \begin{bmatrix} L_{fw} \\ M_{fw} \\ N_{fw} \end{bmatrix} &= \begin{bmatrix} C_{L_b} \\ C_{N_b} \\ C_{M_b} \end{bmatrix} q_b S_b l_b + \begin{bmatrix} C_{L_w} \\ C_{N_w} \\ C_{M_w} \end{bmatrix} q_w S_w c_w \\
 &+ \begin{bmatrix} 0 & -z_{ht} & y_{ht} \\ z_{ht} & 0 & -x_{ht} \\ -y_{ht} & x_{ht} & 0 \end{bmatrix} \begin{bmatrix} X_{ht} \\ Y_{ht} \\ Z_{ht} \end{bmatrix} + \begin{bmatrix} 0 & -z_{vt} & y_{vt} \\ z_{vt} & 0 & -x_{vt} \\ -y_{vt} & x_{vt} & 0 \end{bmatrix} \begin{bmatrix} X_{vt} \\ Y_{vt} \\ Z_{vt} \end{bmatrix}
 \end{aligned} \tag{4}$$

The left side of the formula represents the force and moment provided by the body, wing, Horizontal tail, vertical tail of the aircraft in the body coordinate system.

The aircraft's kinetic equation vector is described below:

$$\begin{aligned}
 \dot{V}_b &= -\omega_{b/n}^b \times V_b + \frac{F_b}{m} + \frac{F_{b,g}}{m} \\
 \dot{\omega}_{b/n} &= J^{-1} \left[M_b - \omega_{b/n}^b \times \left(J \omega_{b/n}^b \right) \right]
 \end{aligned} \tag{5}$$

$$\begin{cases} F_b = F_{gyro} + F_{fw} + F_{pr} \\ M_b = M_{gyro} + M_{fw} + M_{pr} \end{cases} \quad F_{b,g} = \begin{bmatrix} -mgs_0 \\ mgs_\phi c\theta \\ mgc_\phi c\theta \end{bmatrix} \tag{6}$$

3 Attitude Control by Back-Stepping

As a result of the hybrid autogyro model is a strong nonlinear system, we tried PID method, but did not reach the ideal effect. So this paper uses nonlinear control method back-stepping control strategy to design attitude controller and perform the simulation analysis. Back stepping control has the ability of dealing with

mismatched, uncertainties, nonlinear systems [8]. It already showed a great deal of flexibility and superior performance in the design of the robust control of uncertain systems and adaptive control.

In order to use the back-stepping method to control the design, the model of the hybrid autogyro represented by Eq. (5) will be simplified, expressed as a strict feedback form attitude subsystem as shown below:

$$\begin{cases} I_x \ddot{\phi} = \dot{\theta} \dot{\psi} (I_y - I_x) + I_{zx} (\ddot{\psi} + \dot{\theta} \dot{\phi}) + U_2 \\ I_y \ddot{\theta} = \dot{\phi} \dot{\psi} (I_z - I_x) + I_{zx} (\dot{\psi}^2 - \dot{\theta}^2) + U_3 \\ I_z \ddot{\psi} = \dot{\phi} \dot{\theta} (I_x - I_y) + I_{zx} (\ddot{\theta} - \dot{\phi} \dot{\psi}) + U_4 \end{cases} \quad (7)$$

U_2 (roll), U_3 (pitch), U_4 (yaw) are the control variables of three channels. U_1 is the control variable of throttle [9]. By keeping the speed of the aircraft at trim, the throttle control variable U_1 can be obtained. In order to calculate U_2, U_3, U_4 , suppose:

$$\begin{aligned} x_1 = \phi, x_2 = \dot{x}_1 = \dot{\phi}, x_3 = \theta, x_4 = \dot{x}_3 = \dot{\theta}, x_5 = \psi, x_6 = \dot{x}_5 = \dot{\psi}, \\ x_7 = \dot{x}_4 = \ddot{\theta}, x_8 = \dot{x}_6 = \ddot{\psi} \end{aligned}$$

We can get:

$$S_1 : \begin{cases} \dot{x}_1 = x_2 \\ \dot{x}_2 = x_4 x_5 a_1 + (x_8 + x_2 x_4) a_4 + b_1 u_2 \\ \dot{x}_3 = x_4 \\ \dot{x}_4 = x_2 x_6 a_2 + (x_6^2 - x_2^2) a_5 + b_2 u_3 \\ \dot{x}_5 = x_6 \\ \dot{x}_6 = x_2 x_4 a_3 + (x_7 - x_4 x_6) a_6 + b_3 u_4 \end{cases} \quad (8)$$

where:

$$\begin{aligned} a_1 = \frac{I_y - I_z}{I_x}, a_2 = \frac{I_z - I_x}{I_y}, a_3 = \frac{I_x - I_y}{I_z}, a_4 = \frac{I_{zx}}{I_x}, a_5 = \frac{I_{zx}}{I_y}, \\ a_6 = \frac{I_{zx}}{I_z}, b_1 = \frac{1}{I_x}, b_2 = \frac{1}{I_y}, b_3 = \frac{1}{I_z} \end{aligned}$$

The first step: define error variable $z_1 = x_{1d} - x_1$, then:

$$\dot{z}_1 = \dot{x}_{1d} - \dot{x}_1 = \dot{x}_{1d} - x_2 \quad (9)$$

Choose Lyapunov function:

$$\dot{V}(z_1) = z_1 \dot{z}_1 = z_1(\dot{x}_{1d} - x_2) \quad (10)$$

To stabilize z_1 , x_2 is considered a virtual input, express by v_1 :

$$v_1 = \dot{x}_{1d} + \alpha_1 z_1 \quad \alpha_1 > 0 \quad (11)$$

Define the error variable: $z_2 = x_2 - v_1$, then:

$$\dot{V}(z_1) = z_1 \dot{z}_1 = z_1(\dot{x}_{1d} - x_2) = z_1(\dot{x}_{1d} - z_2 - v_1) = -z_1 z_2 - \alpha_1 z_1^2 \quad (12)$$

The coupling part $-z_1 z_2$ will be elimination in the second step.

The second step:

$$z_2 = x_2 - v_1 = x_2 - \dot{x}_{1d} - \alpha_1 z_1 \quad (13)$$

We can get:

$$\dot{z}_1 = -\alpha_1 z_1 - z_2 \quad (14)$$

$$z_2 = x_2 - \dot{x}_{1d} - \alpha_1 z_1 = x_4 x_6 a_1 + (x_8 + x_2 x_4) a_4 + b_1 u_2 - x_{1d} - \alpha_1 (-\alpha_1 z_1 - z_2) \quad (15)$$

Choose Lyapunov function:

$$V(z_1, z_2) = V(z_1) + \frac{1}{2} z_2^2 \quad (16)$$

$$\begin{aligned} \dot{V}(z_1, z_2) &= z_1 \dot{z}_1 + z_2 \dot{z}_2 = -z_1 z_2 - \alpha_1 z_1^2 + z_2 [x_4 x_6 a_1 + (x_8 + x_2 x_4) a_4 \\ &\quad + b_1 u_2 - \ddot{x}_{1d} - \alpha_1 (-\alpha_1 z_1 - z_2)] \\ &= -\alpha_1 z_1^2 + z_2 [-z_1 + x_4 x_6 a_1 + (x_8 + x_2 x_4) a_4 \\ &\quad + b_1 u_2 - \ddot{x}_{1d} - \alpha_1 (-\alpha_1 z_1 - z_2)] \end{aligned} \quad (17)$$

We can design u_2 to make $\dot{V}(z_1, z_2) < 0$:

$$u_2 = \frac{1}{b_1} [-\alpha_2 z_2 + z_1 - x_4 x_6 a_1 - (x_8 + x_2 x_4) a_4 + \ddot{x}_{1d} - \alpha_1 (\alpha_1 z_1 + z_2)] \quad \alpha_2 > 0 \quad (18)$$

Could make:

$$V(z_1, z_2) = -\alpha_1 z_1^2 - \alpha_2 z_2^2 < 0$$

In the same way, we can get:

$$\begin{aligned} u_3 &= \frac{1}{b_2} [-\alpha_4 z_4 + z_3 - x_2 x_6 a_2 - (x_6^2 - x_2^2) a_5 + \ddot{x}_{3d} - \alpha_3 (\alpha_3 z_3 + z_4)] \\ u_4 &= \frac{1}{b_3} [-\alpha_6 z_6 + z_5 - x_2 x_4 a_3 - (x_7 - x_4 x_6) a_6 + \ddot{x}_{5d} - \alpha_5 (\alpha_5 z_5 + z_6)] \end{aligned} \tag{19}$$

4 Simulation and Result Analysis

Give each channel 5° , 10° , -5° step input signal separately, get the response curves as shown in Fig. 4:

It can be seen that the response time of around 0.6 s for θ and 0.4 s for ψ , but the response time of ϕ is a little bigger. Overshoot is not apparent and the steady state error $e_{ss} = 0$ for each channel.

Next, in order to verify that the controller we designed can achieve the desired control effect near the actual flight, we enter the input signal in the actual manual flight test into the simulation model, and each channel's respond as shown in Fig. 5.

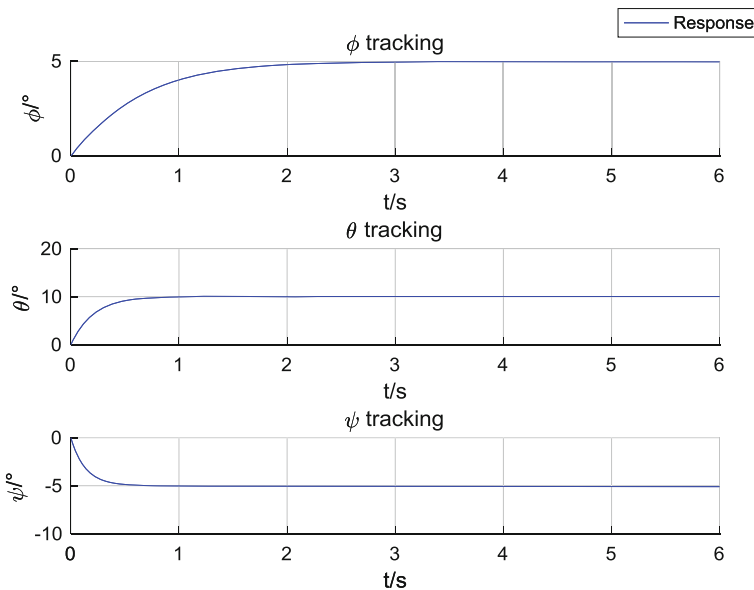


Fig. 4 Step response curve of back-stepping control

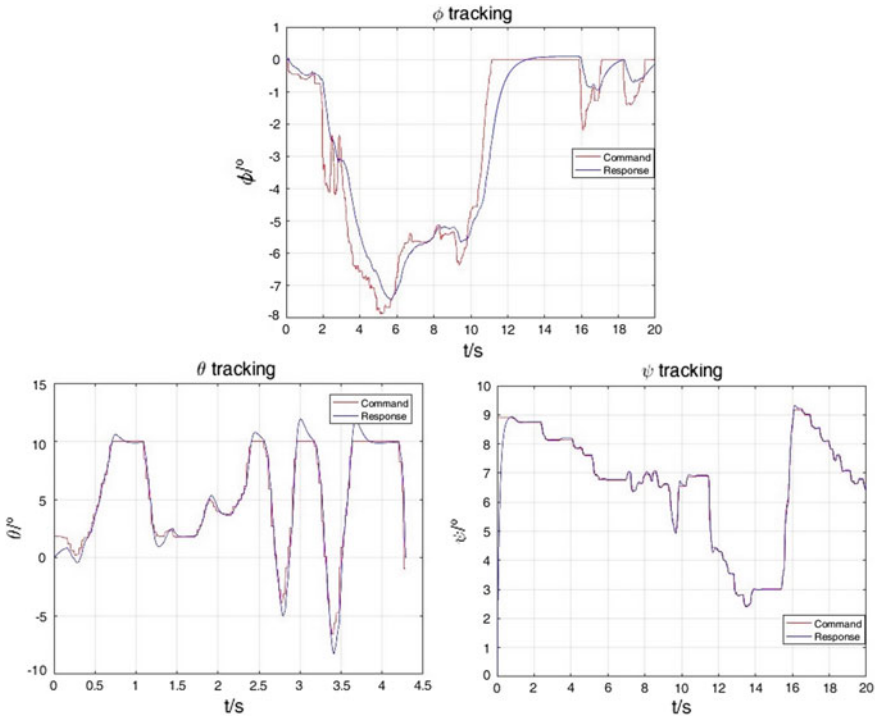


Fig. 5 Roll, pitch and yaw angle tracking curves

The first figure is the roll angle response curve, it can be seen that the controller can successfully track desired roll angles, although it has a command response delay of about 0.5 s. The reason of the response delay should be the adjusting time of ϕ is a little bigger. It may be because the relationship between the control amount of roll U_2 to rotating rotor tilted angle does not accurately reflect the actual situation of the aircraft.

For the pitch and roll channel, we can see the response speed in both curves is very fast and there is no steady-state error or θ response delay, the controller can successfully track desired attitude angles. Compared to the simulation results, the pitch channel has a little overshoot, the parameter of this channel should be improved.

5 Conclusion

In this paper, we focus on the hybrid autogyro, which is a newer type UAV rather than the common UAV. Because the model is more complex, involving the coupling of rotor and fixed-wing, so the modeling encountered a relatively large

difficulty. Finally we use back-stepping control method to design the attitude controller. The controller can successfully control the hybrid autogyro's roll, pitch and yaw angles. Tracking is quick and largely satisfactory, with good stability. There are also some problems in the model and the controller, such as the function between control amount and rotating rotor tilted angle should be improved and the anti-interference ability for the model is poor. So these are the direction of our efforts in the future.

References

1. Leishman JG (2004) Development of the autogyro: a technical perspective. *J Aircr* 41(4): 765–781
2. Prouty RW (2003) Helicopter performance, stability, and control, chapters 1–3. Krieger, London
3. Lin Q (2016) Multi-mode flight control for hybrid V/STOL unmanned aerial vehicle with rotor and wing. PhD Dissertation, School of Automation Science and Electric Engineering, Beihang University, Beijing (in Chinese)
4. Yan K (2016) Research on flight control for hybrid gyroplane UAV. Master's Thesis, School of Automation Science and Electric Engineering, Beihang University, Beijing (in Chinese)
5. Lopez CA, Wells VL (2004) Dynamics and stability of an autorotating rotor/wing unmanned aircraft. *J Guid Control Dyn* 27(2):258–270
6. Mettler B (2003) Identification modeling and characteristics of miniature rotorcraft. Kluwer Academic Publisher
7. Etkin B, Reid LD (1995) Dynamics of flight: stability and control, 3rd edn. John Wiley & Sons, Hoboken, Chapters 2–6
8. Mian AA (2008) Modeling and backstepping-based nonlinear control strategy for a 6 DOF quadrotor helicopter. *Chin J Aerinatics* 03:261–268
9. Das A, Lewis F, Subbarao K (2009) Backstepping approach for controlling a quadrotor using lagrange form dynamics. *J Intell Rob Syst* 56(1–2):127–151